

# Open-Set Domain Adaptation through Self-Supervision

Protopapa Andrea, Quarta Matteo, Ruggeri Giuseppe, Versace Alessandro  
Politecnico di Torino  
Italy

{s286302,s292477,s292459,s292477}@studenti.polito.it <- Riordinare

## Abstract

*In machine learning applications, domain adaptation (DA) techniques try to mitigate the problem of having different domains in the training and test data. Another common problem is represented by the presence of more semantic classes in the test data, which are unknown and completely new to the developed models. The latter problem comes under the name of novelty or anomaly detection. In real world scenarios, it is becoming extremely common suffering of both problems. Open-Set Domain Adaptation (OSDA) methods try to tackle these problems by jointly adapting a model trained on a labeled source domain to an unlabeled target domain while performing novelty detection. We propose a new method leveraging a self-supervised technique, rotation recognition, consisting in first performing novelty detection on the target data and then aligning the two domains avoiding potential negative adaptation. Furthermore, we assess the performance using a new metric which represents in a balanced way the ability to jointly solve the two problems. Experiments conducted on the Office-Home benchmark show interesting results and method effectiveness.*

## 1. Introduction

Nowadays, the widespread usage of deep neural networks to accomplish computer vision tasks has brought huge benefits. In real world applications, as the tasks to cope with are becoming more and more challenging, machine learning methods commonly suffer of a gap between the performance obtained during the development, and the actual performance observed in real usages.

One of the problems which is causing this loss of performance is the domain gap between the training data and the actual observed data. Intuitively, if we train a model on a specific domain, such as employing real world pictures depicting real objects, for example to perform classification, we expect that the model will perform well on a fairly large variety of test cases. However, the actual data present a huge

variety on the domains while still representing the same semantic classes that we want to predict. For example, we may want to be capable of predicting that both an image of a real elephant and a drawing of an elephant are containing the semantic class *elephant*. Domain adaptation techniques have been developing in recent years to reduce the domain gap between a labeled source domain and one or more unlabeled target domains. Generally, this is done by enforcing the learning of domain-invariant patterns of both domains. As underlined in [4], this is usually achieved by learning a transformation function which projects both the source and target domain data in a new space where we jointly maintain the underlying structure of the original data while reducing the domain gap by removing the domain-specific information.

Another big issue encountered in real world usages is the presence of additional anomaly semantic classes on the observed data. The problem comes under the name of *Open-Set Recognition (OSR)* [5], where we require not only to accurately classify the known seen classes, but also effectively deal with unknown ones, which would otherwise drastically weaken the robustness of the methods.

The jointly presence and accounting of the two described problems has been emerged as a new sub-field of computer vision with the name of *Open-Set Domain Adaptation (OSDA)*. As a consequence, if we try to reduce the domain gap between the whole target domain and the source domain, we will observe a negative adaptation due to the unwanted alignment between the data belonging to the anomaly semantic classes and the source classes we want to model and predict. For this reason, it is important to first perform anomaly detection of the additional set of novelty classes, translating the problem into a *Closed-Set Domain Adaptation (CSDA)* one, and next do the alignment between the source and the target domain identified as known.

Common machine learning methods usually leverage huge manually annotated datasets to perform well on the given tasks. However, acquiring annotated material is usually very costly and difficult, moreover, relying on such data may not be scalable in large applications on the long run.

Thus, recently, unsupervised learning techniques are becoming crucial to cope with the aforementioned problems. One of those is self-supervised learning, which consists in creating new automatically labeled data starting from the original unlabeled data. The fundamental idea is creating some auxiliary task from input data so that, by solving such task, the model can learn the underlying structure of the data, for instance high-level knowledge, correlations, and metadata embedded. This type of learning has been recently used for Domain Adaptation, learning robust cross-domain features and supporting generalization [3, 9], and also for some Open Set problems specialized in anomaly detection and discriminating anomalous data [2, 6].

The approach presented in this paper combines the power of the self-supervised learning with the standard supervised learning approach for semantic class recognition. A two-stage method is hence proposed, aiming to identify and isolate unknown class samples in the first stage, before reducing in the second stage the domain gap between the source domain and the known target domain to avoid negative transfer. This is done in both stages using a modified version of the rotation task as self-supervised method, predicting the relative rotation between an image and its rotated version. Finally, a classifier is used to predict if each target sample belongs either to one of the known classes or to an unknown class, being rejected in the latter case. We evaluate the method on the Office-Home benchmark [7] exploiting a new OSDA metric.

To wrap up, our **main contributions** are:

1. we define a new method to tackle OSDA problems which exploits the rotation recognition task to perform both the known/unknown target separation and the domain adaptation;
2. we introduce a new OSDA metric which properly balances the measure of both the performance on predicting the known classes and the performance on doing the unknown rejection;
3. we conduct an extensive ablation over the hyperparameters for different variants of the self-supervised task underlying the benefits of some techniques over others.

## 2. Related Work

## 3. Method

### 3.1. Problem Formulation

Our starting point is the source dataset, defined as  $\mathcal{D}_s = \{(\mathbf{x}_i^s, y_i^s)\}_{i=1}^{N_s} \sim p_s$ , where each element  $\mathbf{x}_i^s$  belonging to class  $y_i^s$  is a sample from the source domain  $S$ . This dataset has a target counterpart,  $\mathcal{D}_t = \{\mathbf{x}_i^t\}_{i=1}^{N_t} \sim p_t$  which is unlabeled instead. In OSDA we have that  $p_s \neq p_t$ . The source

dataset  $\mathcal{D}_s$  is associated with a set of known classes  $\mathcal{C}_s$ , which can also be found in the target dataset  $\mathcal{D}_t$  but is supposedly smaller. In other words,  $|\mathcal{C}_s| < |\mathcal{C}_t|$  and  $\mathcal{C}_s \subset \mathcal{C}_t$ . In domain adaptation, we further have that the target distribution of the known source classes differs from the target distribution of known classes, so  $p_t^s \neq p_s$ . A metric to measure how different two domains are is the openness between source and target domain [1], defined as  $\mathbb{O} = 1 - \frac{C_s}{C_t}$ . When  $\mathbb{O} > 0$ , we're dealing with an OSDA problem.

### 3.2. Approach

The task is split in two separate stages. First, we have to train the model to separate between the known classes ( $\mathcal{C}_s$ ) and the unknown classes ( $\mathcal{C}_{t \setminus s}$ ) in a reliable way. This is achieved via the self-supervised task, training the model to both recognize the class of a sample and its relative orientation. Secondly, we train the model on a union of both source and target datasets, to reject samples when they are not part of the known classes  $\mathcal{C}_s$ .

### 3.3. Rotation Recognition

We denote with  $rot(\mathbf{x}, k)$  the rotation of the sample image  $\mathbf{x}$  by  $k \times 90$  degrees clockwise. This is the self-supervised part of our proposed model as rotation indices  $k \in [0, 3]$  can be randomly generated and then predicted. Relative rotation, meaning that both original and rotated features are supplied to the model, is preferred over just using rotated features as some objects might not have an absolute correct orientation. Alternatively, instead of having the model predict the rotation of a sample for any class using the same classifier, we also try using a different head for each one of the known classes  $\mathcal{C}_s$ .

### 3.4. Step I: Sample Separation

Separating samples requires iterating over  $\tilde{\mathcal{D}}_s = \{(\mathbf{x}_i^s, \tilde{\mathbf{x}}_i^s, z_i^s)\}_{i=1}^{N_s}$ , where  $\tilde{\mathbf{x}}_i^s$  is the  $z_i^s \times 90$  degrees rotated version of  $\mathbf{x}_i^s$ . The network is composed by an extractor  $E$  and two classifiers,  $R_1$  and  $C_1$ .  $C_1$  is the object classifier, assigning image labels  $\hat{y}_i^s \in \{0, \dots, |\mathcal{C}_s|\}$ , while  $R_1$  is the relative rotation classifier, assigning rotation indices  $\hat{z}_i^s \in [0, 3]$ .  $\tilde{\mathbf{z}}_i^s$  and  $\tilde{\mathbf{y}}_i^s$  are the vector representations of  $\hat{z}_i^s$  and  $\hat{y}_i^s$ . The multi-head rotation classifier uses  $|\mathcal{C}_s|$  heads for the rotation task. In this case, which head to use during separation is up to the object classifier  $C_1$ . Object predictions are made as  $\tilde{\mathbf{x}}_i^s = \text{softmax}(E(\mathbf{x}_i^s))$ , while relative rotation predictions are computed as  $\tilde{\mathbf{z}}_i^s = \text{softmax}(R_1([E(\mathbf{x}_i^s), E(\tilde{\mathbf{x}}_i^s)]))$ . If a multi-head rotation classifier is used, the  $j = y_i^s$  head is used as  $\tilde{\mathbf{z}}_i^s = \text{softmax}(R_{1,j}[E(\mathbf{x}_i^s), E(\tilde{\mathbf{x}}_i^s)])$ . The model is trained to minimizing the objective function  $\mathcal{L}_1 = \mathcal{L}_{C_1} + \mathcal{L}_{R_1}$ . This is the sum of two cross-entropy loss functions:

$$\mathcal{L}_{C_1} = - \sum_{i \in \mathcal{D}_s} \mathbf{y}_i^s \log \tilde{\mathbf{y}}_i^s \quad (1)$$

$$\mathcal{L}_{R_1} = -\alpha_1 \sum_{i \in \tilde{\mathcal{D}}_s} \mathbf{y}_i^s \log \tilde{\mathbf{z}}_i^s \quad (2)$$

Where  $\alpha_1$  is a weight associated to the rotation task. We also try using an extended rotation loss function  $\mathcal{L}_{R_1}^*$  implementing an additional center loss [8] term:

$$\mathcal{L}_{R_1}^* = -\alpha_1 \sum_{i \in \mathcal{D}_s} \mathbf{y}_i^s \log \tilde{\mathbf{z}}_i^s + \lambda_1 \|\mathbf{v}_i^s - \gamma(\mathbf{z}_i^s)\|_2^2 \quad (3)$$

Here  $\mathbf{v}_i$  is the penultimate layer of the rotation classifier, called features,  $\gamma(\mathbf{z}_i)$  is the center of the features associated to class  $i$ ,  $\|\cdot\|_2^2$  is the  $l_2$  norm and  $\lambda_1$  is the weight associated with the center loss term.

When training is completed, we can start separating samples. To do so, normality scores  $\mathcal{N}(\cdot)$  are used, defined as the maximum prediction of the rotation classifier:  $\mathcal{N}(\tilde{\mathbf{x}}_i) = \max(\tilde{\mathbf{z}}_i)$ . To predict whether a sample belongs to the known samples of the target domain  $\mathcal{D}_t^{knw}$  or the unknown ones  $\mathcal{D}_t^{unk}$  requires picking a threshold  $\tilde{\mathcal{N}}$ . The separation is then done as:

$$\begin{cases} \mathbf{x}_i^t \in \mathcal{D}_t^{knw} & \text{if } \mathcal{N}(\tilde{\mathbf{x}}_i^t) \geq \tilde{\mathcal{N}} \\ \mathbf{x}_i^t \in \mathcal{D}_t^{unk} & \text{if } \mathcal{N}(\tilde{\mathbf{x}}_i^t) < \tilde{\mathcal{N}} \end{cases} \quad (4)$$

When using a multi-head rotation classifier, it is required to choose among the  $|\mathcal{C}_s|$  possible heads to make the prediction. Head  $R_{1,j}$  is used by choosing  $j$  as  $j = \arg \max_j \tilde{\mathbf{y}}_i^t$ .

### 3.5. Step II: Domain Alignment

In this phase, we build two "new" datasets. The first one is  $\mathcal{D}_s^*$ , composed as  $\mathcal{D}_s \cup \mathcal{D}_t^{unk}$ . Since  $\mathcal{D}_t$  is an unlabeled dataset but  $\mathcal{D}_s$  is a labeled one, samples in  $\mathcal{D}_t^{unk}$  are labeled as unknowns. The second one is  $\mathcal{D}_t^{knw}$ . Here we also use two new classifiers,  $C_2$  and  $R_2$ , similarly to how they were used in the first phase but with  $C_2$  predicting  $|\mathcal{C}_s| + 1$  classes to accommodate unknown predictions. In this step  $R_2$  is always single-headed and has its own weight  $\alpha_2$ . The objective function is the same described in equations 1 and 2. The main difference here is that  $C_2$  is actually trained to recognize unknown classes, on both domains.

### 3.6. Performance Metrics

Evaluating model performance requires finding a balance between two values:  $OS^*$ , the fraction of correctly classified samples, and  $UNK$ , the fraction of correctly rejected samples. A model not confident enough to reject a sample could still achieve high  $OS^*$  values but near-zero  $UNK$ , while a model rejecting every sample as unknown will

achieve perfect  $UNK$  and zero  $OS^*$ . To compare models we use the harmonic mean between  $OS^*$  and  $UNK$ , defined as  $HOS = 2 \frac{OS^* \times UNK}{OS^* + UNK}$ . This is because this kind of mean tends to give a bigger weight to the smaller values, resulting in a more severe evaluation of models.

## 4. Experiments

### 4.1. Dataset

Our model is tested on the *Office-Home* dataset [7], which features 65 classes of images over four different domains: Art (A), Clipart (C), Product (P) and Real World (R). We set the first 45 classes to be known while the remaining 20 are unknown. For each experiment, we report both the best achieved HOS as well as the last reported HOS. As separation is crucial for the model effectiveness, we also report the computer AUROC score for the first part.

### 4.2. Results

Table 1 contains the results for all 12 (**ne abbiamo provati davvero 12???**) available domain shifts, as well as performance differences when using multi-head rotation classifiers and center loss. Further details are to be found in section 5. We can notice that multi-headed models are more capable of correctly discriminating between known and unknown samples, ultimately resulting in better domain alignment. A further advantage is given when combined with center loss. AUROC values are computed at the end of the separation stage, while HOS values are sampled at regular times on the entire original target dataset.

## 5. Implementation Details

### 5.1. Model Parameters

All models were run using stochastic gradient descent with batch size 32, a weight decay of 0.0005 and momentum of 0.9. For single-headed models, a base learning rate of 0.001 is used, while for multi-headed models it is set to 0.003. This is because only one head of the heads is trained with each sample, so the process needs to be sped up. Rotation classifier use a learning rate set to a tenth of the base learning rate. A step learning rate scheduler is used, reducing it by a factor of 10 after 90% of epochs. All models are run for 50 epochs for the first step described in 4 and for 25 epochs for the second step described in 3.5. For model using the center loss a centroid learning rate of 0.5 is used. All other parameters are configuration-specific and are reported in table 2. "No Rotation" model is the same as a single-head without center loss model with  $\alpha_2 = 0$ .

*Extractor E:* The extractor employed is a ResNet-34[Inserire cit a ResNet] è pretrained??? ma 34 o 18??? for all classifiers.

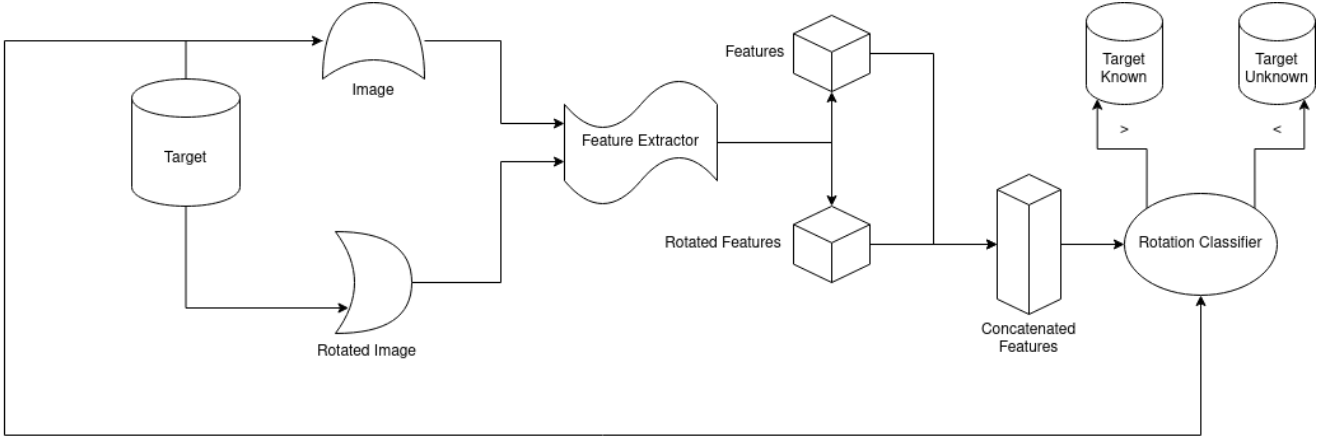


Figure 1. Schema representing the target images separation process

Single-Head, CE Loss				
Source	Target	AUROC	HOS	HOS*
S	T	50%	30%	30%
S	T	50%	30%	30%
S	T	50%	30%	30%
Multi-Head, CE Loss				
Source	Target	AUROC	HOS	HOS*
S	T	50%	30%	30%
S	T	50%	30%	30%
S	T	50%	30%	30%
Single-Head, CE+C Loss				
Source	Target	AUROC	HOS	HOS*
S	T	50%	30%	30%
S	T	50%	30%	30%
S	T	50%	30%	30%
Multi-Head, CE+C Loss				
Source	Target	AUROC	HOS	HOS*
S	T	50%	30%	30%
S	T	50%	30%	30%
S	T	50%	30%	30%
No Rotation				
Source	Target	AUROC	HOS	HOS <sub>Best</sub>
S	T	50%	30%	30%
S	T	50%	30%	30%
S	T	50%	30%	30%

Table 1. Results for domain alignment. AUROC is the area under the ROC. HOS is latest achieved HOS, HOS\* the best achieved through all epochs.

*Classifier  $C_1, C_2$ :*  $C_1$  is composed of a 45 dimensional output. All unknown samples are mapped as belonging to class 45.  $C_1$  is used as a starting point for  $C_2$ . As no unknowns are present on the source dataset (they are

MH	CL	$\alpha_1$	$\alpha_2$	$\lambda_1$	$\tilde{\mathcal{N}}$
Off	Off	0.0	0.0	0.0	0.0
On	Off	0.0	0.0	0.0	0.0
Off	On	0.0	0.0	0.0	0.0
On	On	0.0	0.0	0.0	0.0

Table 2. Model Parameters

removed), the weight of unknown samples in the second step is set to **spiegare come è bilanciato** while for all other classes it is set to 1. A single fully connected layer  $512 \rightarrow 45$  with batch-norm is used.

*Classifier  $R_1, R_2$ :*  $R_1$  and  $R_2$  are composed by a  $1024 \rightarrow 256$  and a  $256 \rightarrow 4$  fully connected layers, named *Discriminators*. The 256-dimensional output are the features used by the center loss for inferring class centers. If multi-head is used, each head is a separate discriminator.  $R_2$  is always a single-head classifier, even if using a multi-head rotation classifier.

## 5.2. Ablation Study

As shown in table 1 different architectures give different results, and as shown in table 2 each one requires a different set of parameters. To choose optimal parameters a sequential approach is followed, by optimizing one parameter at the time. The order of optimization followed is:  $\alpha_1, \lambda_1, \tilde{\mathcal{N}}, \alpha_2$ . Models not using center loss just skip the  $\lambda_1$  optimization. Ablation study were run on two domain shifts, Art  $\rightarrow$  Clipart and Clipart  $\rightarrow$  Product. In table ?? we report the steps followed. All other settings follow what is reported in 5.1. The result here obtained are the same reported in table 2.

MH OFF CL OFF				
$\alpha_1$	$\tilde{\mathcal{N}}$	$\alpha_2$	AUROC	HOS <sub>mean</sub>
Picking $\alpha_1$				
1.0	0.5	3.0	0.5	30%
3.0			0.5	30%
5.0			0.5	30%
10.0			0.5	30%
Picking $\tilde{\mathcal{N}}$				
1.0	0.40	3.0	0.5	50%
	0.50		0.5	50%
	0.55		0.5	50%
	0.60		0.5	50%
Picking $\alpha_2$				
1.0	0.6	1.0	0.5	50%
		3.0	0.5	50%
		5.0	0.5	50%
		10.0	0.5	50%
Final Parameters				
1.0	0.6	3.0	0.5	50%

Table 3. Ablation performed for OFF-OFF configuration

- [8] Yandong Wen, Kaipeng Zhang, Zhifeng Li, and Yu Qiao. A discriminative feature learning approach for deep face recognition, 2016. 3
- [9] Jiaolong Xu, Liang Xiao, and Antonio M. Lopez. Self-supervised domain adaptation for computer vision tasks. 2019. 2

## 6. Future Work

The results show that self-supervision technique can help in domain adaptation task and open-set classification tasks. A few critical points still remain on our method of study and proposed solution. The most important one is probably parameter choosing for different models, as we have seen that variations cause huge differences in results and sequential optimization of parameter is a sub-optimal heuristic. Furthermore, having the model to learn two different tasks at once, it could be useful to use a slower learning model at the expense of longer training times.

## References

- [1] Abhijit Bendale and Terrance Boult. Towards open set deep networks, 2015. 2
- [2] Liron Bergman and Yedid Hoshen. Classification-based anomaly detection for general data, 2020. 2
- [3] Fabio Maria Carlucci, Antonio D’Innocente, Silvia Bucci, Barbara Caputo, and Tatiana Tommasi. Domain generalization by solving jigsaw puzzles, 2019. 2
- [4] Abolfazl Farahani, Sahar Voghoei, Khaled Rasheed, and Hamid R. Arabnia. A brief review of domain adaptation, 2020. 1
- [5] Chuanxing Geng, Sheng-Jun Huang, and Songcan Chen. Recent advances in open set recognition: A survey. 2021. 1
- [6] Izhak Golan and Ran El-Yaniv. Deep anomaly detection using geometric transformations. 2018. 2
- [7] Hemanth Venkateswara, Jose Eusebio, Shayok Chakraborty, and Sethuraman Panchanathan. Deep hashing network for unsupervised domain adaptation, 2017. 2, 3